Biochimica et Biophysica Acta 1840 (2014) 2070–2079

Contents lists available at ScienceDirect

Biochimica et Biophysica Acta

journal homepage: www.elsevier.com/locate/bbagen

Post-transcriptional regulation of the creatine transporter gene: Functional relevance of alternative splicing

Joseph D.T. Ndika [a,b], Cristina Martinez-Munoz [a], Nandaja Anand [a], Silvy J.M. van Dooren [a], Warsha Kanhai [a], Desiree E.C. Smith [a], Cornelis Jakobs [a], Gajja S. Salomons [a,b,c,*]

[a] Department of Clinical Chemistry, Metabolic Unit, VU University Medical Center, Amsterdam, The Netherlands
[b] Neuroscience Campus, VU University Medical Center, Amsterdam, The Netherlands
[c] Department of Clinical Genetics, VU University Medical Center, Amsterdam, The Netherlands

ARTICLE INFO

Article history:
Received 28 May 2013
Received in revised form 7 February 2014
Accepted 12 February 2014
Available online 20 February 2014

Keywords:
Na^+/Cl^- cotransporter
Creatine transporter
Alternative splicing
Creatine uptake upregulation
Intellectual disability

ABSTRACT

Background: Aberrations in about 10–15% of X-chromosome genes account for intellectual disability (ID); with a prevalence of 1–3% (Gécz et al., 2009 [1]). The *SLC6A8* gene, mapped to Xq28, encodes the creatine transporter (CTR1). Mutations in *SLC6A8*, and the ensuing decrease in brain creatine, lead to co-occurrence of speech/language delay, autism-like behaviors and epilepsy with ID. A splice variant of *SLC6A8*–*SLC6A8C*, containing intron 4 and exons 5–13, was identified. Herein, we report the identification of a novel variant — *SLC6A8D*, and functional relevance of these isoforms.
Methods: Via (quantitative) RT-PCR, uptake assays, and confocal microscopy, we investigated their expression and function vis-à-vis creatine transport.
Results: SLC6A8D is homologous to *SLC6A8C* except for a deletion of exon 9 (without occurrence of a frame shift). Both contain an open reading frame encoding a truncated protein but otherwise identical to CTR1. Like *SLC6A8*, both variants are predominantly expressed in tissues with high energy requirement. Our experiments reveal that these truncated isoforms do not transport creatine. However, in *SLC6A8* (CTR1)-overexpressing cells, a subsequent infection (transduction) with viral constructs encoding either the *SLC6A8C* (CTR4) or *SLC6A8D* (CTR5) isoform resulted in a significant increase in creatine accumulation compared to CTR1 cells re-infected with viral constructs containing the empty vector. Moreover, transient transfection of CTR4 or CTR5 into HEK293 cells resulted in significantly higher creatine uptake.
Conclusions: CTR4 and CTR5 are possible regulators of the creatine transporter since their overexpression results in upregulated CTR1 protein and creatine uptake.
General significance: Provides added insight into the mechanism(s) of creatine transport regulation.

1. Introduction

Genetic deficiencies involving *AGAT* (OMIM ID: 602360), *GAMT* (OMIM ID: 601240) or *SLC6A8* (OMIM ID: 300036), make up the creatine deficiency syndromes — a group of inborn errors of metabolism with symptoms such as intellectual disability, autism-like behavior and epilepsy [2–4]. Intellectual disability, with a prevalence of 1-3% [1], is also the main symptomatic of defective creatine synthesis or transport. Creatine supplementation is the main therapeutic approach, with success (notably improved cognitive function) in treating AGAT and GAMT deficiencies [5]. The poor permeability of the blood–brain barrier to creatine (reviewed in [6]) renders creatine supplementation ineffective for treating *SLC6A8* deficiency. A recent comprehensive overview of creatine metabolism and transport in relation to CNS function is reviewed in Braissant et al. [45]. Congenital creatine deficiency aside, creatine has also been used to treat mitochondrial and muscular diseases, to alleviate brain and spinal cord injuries and to improve mental performance [7]. Creatine has also been employed as a neuroprotective agent in animal models of Parkinson's and Huntington's diseases [8]. In a more recent study [9], overexpression of the creatine transporter in mice resulted in protection against acute myocardial infarction. Consequently insight into the mechanisms of how the transporter is regulated is valuable.

Alternative splicing is one of the most important mechanisms regulating gene expression. It enables diversification of one gene into different protein products and is thought to provide a molecular mechanism for fine-tuning the gene functions of a single locus [10,11]. Contrary to the expected minor role of alternative splicing in functional regulation, large scale sequencing- and bioinformatics-based studies have reported that it occurs in up to 94% of human genes [12,13]. The presence of a novel *SLC6A8* splice variant (*SLC6A8C*), was revealed in primary fibroblasts of different individuals and in different human tissues [14]. The authors were however unable to detect *SLC6A8B* (GenBank: U17986) — the first identified splice variant

* Corresponding author at: Metabool Lab, PK 1X 009, De Boelelaan 1117, 1081HV Amsterdam, The Netherlands. Tel.: +31 204443053.
E-mail address: g.salomons@vumc.nl (G.S. Salomons).

http://dx.doi.org/10.1016/j.bbagen.2014.02.012
0304-4165/

of *SLC6A8*. In the present study, we report the identification in human and mouse, of a new variant (*SLC6A8D*) of presumably the *SLC6A8C* mRNA, with an in-frame deletion of exon 9. In order to investigate the functional relevance of alternative splicing of *SLC6A8* in terms of creatine uptake and/or regulation of the full-length creatine transporter, we generated recombinant mouse 3T3 Swiss cells overexpressing each splice variant, the full length transporter, as well as cells co-expressing the full length transporter with either one or the other splice isoform.

2. Materials and methods

2.1. Identification of SLC6A8D transcript

Total RNA was extracted (RNA isolation kit; Promega) from HEK-293 cells (since *SLC6A8* expression is high in kidney) and from primary human fibroblasts obtained from both controls and a patient with a genomic deletion encompassing the entire *SLC6A8* gene. cDNA synthesis (Fermentas) was performed (with and without reverse transcriptase, to check for gDNA contamination) using 1 μg of RNA. A forward primer complementary to intron 4 and a reverse primer complementary to the 3′UTR of the *SLC6A8* locus were designed to amplify both *SLC6A8C* and *SLC6A8D* from HEK293 cDNA (Table 1, №. 1). Subsequently nested primers were used to detect presence of *SLC6A8C* and *SLC6A8D* transcripts in the amplified PCR products. *SLC6A8D*-specific primers were designed complementary to intron 4 and spanning exon 8/10 such that only messages lacking exon 9 will be amplified (Table 1, №. 2). For detection of specific *SLC6A8C* and *SLC6A8* transcripts, previously designed primers [14] were used (Table 1, №. 3 and №. 4). RT-PCR of all transcripts was performed using KAPA HiFi™ Hotstart DNA polymerase with GC buffer (Kapa Biosystems). The general PCR conditions used were as specified by the manufacturer, except for the inclusion of 0.2 M Betaine in each reaction. Thermocycling was as follows: initial denaturation for 5 min at 95 °C; followed by 38 cycles of 20 s at 98 °C, followed by 15 s at 66 °C (*SLC6A8*, *SLC6A8C*, *SLC6A8D*) or 61 °C (*GAPDH*), and 2 min at 72 °C; with a final extension step of 10 min at 72 °C. Transcript identities were confirmed by sequencing (ABI 3130XL Genetic Analyser; Applied Biosystems).

2.2. Detection of SLC6A8D expression in monkey and mouse

Slc6a8d expression in mouse was investigated in NIH-3T3 2.2 fibroblasts and primary mouse embryonic fibroblasts (MEFs) of FVB mice. Two monkey cell lines (CP132 and Vero) were also included. RT-PCR for the monkey cell lines was performed with same primers and PCR conditions as for the human samples. For screening of the mouse cells, the primers were specifically designed to amplify mouse *slc6a8*-derived sequences (Table 1, №. 6, №. 7, №. 8); consequently the PCR annealing temperature (Ta) was adjusted to 61 °C for *slc6a8d*. As control, amplification of *Slc6a8c* and *Slc6a8* (Ta, 59 °C) was included. All PCR products were gel-purified and sequenced.

2.3. Quantitative real-time PCR (Q-PCR)

Investigation of differential splice variant expression was carried out on RNA isolated from 20 different tissues (FirstChoice™ Human Total RNA survey panel; Ambion). Gene-specific primers and probes used for amplification of each transcript are shown in Table 2.

To investigate if upregulation of creatine uptake in 3T3 Swiss cells co-expressing CTR1 with a splice isoform compared to cells co-expressing CTR1 with an empty vector, was as a result of enhanced *SLC6A8* transcription, standard Q-PCR was performed on an ABI7300 (Applied Biosystems) using a probe (5′-FAM 3′-TAMRA labeled probe: 5′-TGGGTGCTGGTCTACT TCTGTGTC-3′) and primers (5′-AAGTCTTGAGGCTGTCTGG-3′ and 5′-ACGATCTTTCCCGTGGAT-3′) specific for exon 4 of human *SLC6A8*.

All reactions were performed in the presence of 1 M Betaine and ROX reference dye, and corrected for input by normalizing to *GAPDH* (human tissues) or *Gapdh* (mouse 3T3 Swiss cells) gene expression assay (PrimeTime™ Std qPCR Assay; IDT Technologies). Quantification (threshold cycle number, C_T) of both target and reference genes was carried out in triplicate and in independent wells using the $2^{-\Delta Ct}$ method. Analysis was done using the Q-Gene™ software package [15]. The mean normalized expression was obtained by averaging the C_T values of target and reference genes, respectively and subsequent calculation of the standard error of the mean normalized expression [16].

2.4. Construction of pBABE-hygro-SLC6A8-EGFP, pBABE-puro-SLC6A8C-EGFP and pBABE-puro-SLC6A8D-EGFP expression vectors

The open reading frame (ORF) of all isoforms was cloned in-frame to the N-terminal of EGFP (enhanced green fluorescent protein). In order to obtain a *pBP-SLC6A8D-EGFP* construct; RNA was isolated from HEK293 cells followed by cDNA synthesis. The ORF of *SLC6A8D* (exons 7–13) was amplified by RT-PCR using primers with *HindIII* and *EcoRI* restriction site overhangs (Table 1, №. 9), and then cloned into pEGFPN1 by standard cloning techniques. Via PCR (Table 1, №. 11) and site directed mutagenesis, an *EcoRI-SLC6A8D-EGFP-SalI* construct was then shuttled from its pEGFPN1 vector into a *pBABE-puro* (pBP) destination vector. The ORFs

Table 1
PCR and cloning primers.

No.	Species	Forward/reverse sequence	mRNA sequence	*SLC6A8* location	Amplicon size (bp)
1	Human	5′-GAGGTACTGAAAGCCAAGCAATGC-3′ 5′-GCTGGTGATGTGAGCTGAGT-3′	*SLC6A8C/SLC6A8D*	Intron 4 3′ UTR	1969/1831
2	Human/monkey	5′-CTCCCACACCTGCACTGCCC-3′ 5′-GACGTACATCCCGCCCTGGC-3′	*SLC6A8D*	Intron 4 Exon 8/10	827
3	Human/monkey	5′-CTCCCACACCTGCACTGCCC-3′ 5′-GGAGAGATCGATGACAAAGCAG-3′	*SLC6A8C*	Intron 4 Exon 9	938
4	Human/monkey	5′-ATGGCGAAGAAGAGCGCCGAG-3′ 5′-GCTGGTGATGTGAGCTGAGT-3′	*SLC6A8*	Exon 1 3′ UTR	1930
5	Human	5′-ATGGCGAAGAAGAGCGCCGAG-3′ 5′-GCTGGTGATGTGAGCTGAGT-3′	*GAPDH*		819
6	Mouse	5′-CAAGAATGATCTGGAGTTTGGG-3′ 5′-GACGTACATTCCACCCTGGC-3′	*Slc6a8d*	Intron 4 Exon 8/10	944
7	Mouse	5′-CAAGAATGATCTGGAGTTTGGG-3′ 5′-GGAGAGATCGATGACAAAGCAG-3′	*Slc6a8c*	Intron 4 Exon 9	1056
8	Mouse	5′-GGTATCTATAGCGTGTCTGG-3′ 5′-TTACATGACACTCTCCACCACG-3′	*Slc6a8*	Exon 2 Exon 13	1884
9	Human	5′-CCCAAGCTTCCACCATGGCTGCAGAGCAGGGCGTGC-3′ 5′-CGGAATTCGCATGACACTCTCCACCACG-3′	*SLC6A8C/SLC6A8D*	Exon 7 Exon 13	809/671
10	Human	5′-CGGGATCCACCATGGCGAAGAAGAGC-3′ 5′-CGGGATCCCATGACACTCTCCACCACG-3′	*SLC6A8*	Exon 1 Exon 13	1905
11	Recombinant	5′-CGCGAATTCCACCATGGCTGCAGAGCAGGGCGTGC-3′ 5′-CGCGTCGACCTCTACAAATGTGGTATGGCTG-3′	*SLC6A8C-/SLC6A8D-(EGFP)*	Exon 7	1650/1515

Table 2
Q-PCR primer pairs and probes. To quantify *SLC6A8C* transcripts, cDNA synthesis was carried out with a primer in exon 9 (to distinguish *SLC6A8C* from *SLC6A8D*) followed by PCR with *SLC6A8C*-specific primers. To quantify *SLC6A8* and *SLC6A8D* transcripts, cDNA synthesis was done with an oligo(dT) primer followed by qPCR with gene-specific primers.

	Gene		
	SLC6A8	*SLC6A8C*	*SLC6A8D*
cDNA synthesis	$Oligo(dT)_{20}$	5′-GGAGAGATCGATGACAAAGCAG-3′	$Oligo(dT)_{20}$
Forward primer (10 μM)	5′-CAGCATCAATGTCTGGAACA-3′	5′-GGGACCTCTGAACATACCT-3′	5′-GACAGCCAGGGCGGGAT-3′
Reverse primer (10 μM)	5′-GCCAGCACCATGATGTAGTA-3′	5′-GCAGTGAAGTACACGATCTG-3′	5′-ACCACGCACTCCCAAAAG-3′
Probe (5 μM) 5′Fam, 3′Tamra	5′-TCAAAGGCCTGGGCTACGCCT-3′	5′-ACAGCCTCCGCTGAGCAGCCT-3′	5′-ACTACTCGGCCAGCGGCACCA-3′

of *SLC6A8* and *SLC6A8C* were cloned previously in-frame with EGFP in a pEGFPN1 plasmid [14,17]. A *BamHI-EGFP-SalI* restriction-enzyme-digested fragment was isolated from pEGFPN1 and re-cloned into both *pBABE-hygro* (pBH) and pBP vectors. Via PCR (Table 1, №. 10) a *BamHI-SLC6A8-BamHI* fragment was obtained from pEGFPN1-*SLC6A8* and re-cloned in-frame to EGFP in pBH to produce pBH-*SLC6A8*-EGFP. A pBP-*SLC6A8C*-EGFP construct was generated by shuttling a PCR-generated *EcoRI-SLC6A8C*-EGFP-*SalI* fragment from *SLC6A8C*-pEGFPN1 into a pBP vector. Integrity of all clones was verified by sequencing.

2.5. Generation of recombinant viruses

Viruses containing the empty vectors (*pBP-EGFP* or *pBH-EGFP*), the truncated isoforms (*pBP-SLC6A8C-EGFP* or *pBP-SLC6A8D-EGFP*) and the full-length transporter (*pBH-SLC6A8-EGFP*) constructs were generated. pBP and pBH vectors have the viral packaging signal sequence (Psi) while Phoenix cells (HEK293T) express viral GAG-POL and ENV genes. Transfection of these Phoenix producer cell lines with pBP/pBH-based vectors yields viral supernatants with an ecotropic host range. Phoenix cells were cultured under standard mammalian cell culture conditions to 70% confluence in DMEM cell culture medium (GIBCO, Scotland) supplemented with 1% pen/strep, 1% L-glutamine and 10% FBS. They were subsequently transfected ($CaCl_2$/HBS method; Sigma) with 25 μg endotoxin-free plasmid DNA (Nucleobond™ 500 EF Kit; Bioke). Transfection efficiency was monitored via EGFP fluorescence. 48 and 72 h after transfection, 10 ml of medium containing recombinant viruses was tapped, filtered, flash-frozen in liquid nitrogen and stored at −80 °C.

2.6. Infection of 3T3 Swiss mouse fibroblast cells with construct-containing viruses

In a first round of infections two “primary” cell lines were generated expressing either the empty vector (*pBH-EGFP*) or CTR1 (*pBH-SLC6A8-EGFP*) with hygromycin resistance as a selectable marker. Next, these two cell lines were re-infected (in duplicate, here-in called *Infection I* and *Infection II*) with *pBP-EGFP-*, *pBP-SLC6A8C-EGFP-* or *pBP-SLC6A8D-EGFP*-containing viruses with puromycin resistance as the co-selectable marker. Thus in total duplicates of 6 cell lines were generated co-expressing; the two empty vectors (*1. pBH-EGFP/pBP-EGFP*), one splice variant with an empty vector (*2. pBH-EGFP/pBP-SLC6A8C-EGFP* or *3. pBH-EGFP/pBP-SLC6A8D-EGFP*), *SLC6A8* with an empty vector (*4. pBH-SLC6A8-EGFP/pBP-EGFP*), *SLC6A8* with a splice variant (*5. pBH-SLC6A8-EGFP/pBP-SLC6A8C* or *6. pBH-SLC6A8-EGFP/pBP-SLC6A8D-EGFP*). The infections were carried out as follows; 3T3 Swiss cells were cultured (same medium and conditions as above) to 50% confluence. Next, individual viral taps were thawed to 37 °C and mixed. Cell growth medium was refreshed with virus-containing supernatant (5 ml/10 cm dish, supplemented with 4 μg/ml polybrene). A non-infected control plate was taken along. 24 h post infection; successful transformants were selected by addition of 250 μg/ml hygromycin for 5 days (or 7 μg/ml puromycin + 125 μg/ml hygromycin for 3 days, 24 h after the second round of infections). After the hygromycin-based infection, stable transformed cells were maintained for 7 days in 125 μg/ml hygromycin until the puromycin-based infections. Following the second selection, cell populations were recovered in 3.5 μg/ml puromycin- and 125 μg/ml hygromycin-supplemented medium. 24 h prior to creatine uptake assays, recombinant 3T3 Swiss cells were seeded to 70% confluence in medium without antibiotics. 4 replicates per infected cell line were seeded − 3 for creatine uptake and 1 plate to make pellets for both Western blot and Q-PCR. Cell pellets were flash-frozen in liquid nitrogen, and stored at −80 °C until further use.

2.7. Creatine uptake assay

Prior to incubation of the cells in creatine, intracellular amino acids were depleted, based on a previously described method [18]. Briefly; recombinant cells were incubated for 1 h at 37 °C in Earle's Balanced Salts (EBSS; Sigma-Aldrich) supplemented with 0.1% D-glucose and 0.25% BSA. Cell monolayers were washed with EBSS and incubated (5 min for 48 h; 95% air/5% CO_2 at 37 °C) in DMEM (10% FBS, 1% Pen/Strep, 1% L-Glu) with the desired amount [5 μM (5 μmol/l)–2000 μM (2000 μmol/l)] of stable-isotope-labeled creatine-[methyl-^{13}C] monohydrate. Uptake was stopped by rapidly washing cells with cold Hank's Balanced Salt Solution (HBSS). The cells were harvested (2 min at 37 °C in 0.05% Trypsin + EDTA, GIBCO; Scotland), resuspended in cold HBSS followed by centrifugation (5 min, 1400 rpm).

Cell pellets were resuspended in Milli-Q grade water and disrupted by vortexing. After centrifugation (1 min, 12,000 rpm), the supernatant was cleaned further on an Amicon Ultra − 10 K membrane. Measurement of creatine-[methyl-^{13}C] was performed on the protein-free eluate, using creatine-[$^2H_3$] (Sigma-Aldrich) as internal standard. In parallel, protein content was determined from a fraction of the disrupted cells using a bicinchoninic acid protein assay kit, according to the instructions of the manufacturer (Sigma-Aldrich). Creatine concentration is expressed as pmol creatine/μg total protein. Measurements were performed on an API 3000 triple quadruple tandem mass spectrometer (Applied Biosystems) with a Perkin-Elmer Series 200 HPLC pump and a Perkin-Elmer Series 200 auto sampler (operated at 4 °C). Using a Symmetry Shield RP18 analytical column (3.0 × 100 mm; 3.5 μm; Waters) 10 μl of the sample was separated using 5 mM nonapentanoic acid as an ion-pair reagent. In 5 min the acetonitrile content was linearly increased from 5% to 15%, and subsequently in 5 min from 15% to 50%. The flow rate was 0.3 ml/min. The turbo ion electrospray was operated in positive ion mode, the cone temperature was set to 450 °C and the cone voltage was 5000 V. Nitrogen was used as the turbo ion gas at a flow rate of 8 l/min. Collision induced dissociation was initiated using nitrogen as the collision gas at a pressure of 0.06 kPa. Creatine was fragmented with a collision energy of 35 V. The following MS/MS transitions were measured (creatine; 132.0 → 90.0, creatine-[methyl-^{13}C]; 133.0 → 91.0 and creatine-[$^2H_3$]; 135.0 →93.0). The LC–MS/MS data were acquired and processed using Analyst for Windows software (Applied Biosystems). The limit of quantification (S/N = 10) was estimated to be 20 pmol.

2.8. Western blot

Cell pellets were lysed in urea lysis buffer (8 M urea/100 mM NaCl/10 mM Tris–HCL, pH 8.0). Protein concentrations for each sample were determined as described above and normalized to equal concentrations with additional lysis buffer and SDS sample buffer.

Cell lysates (40 μg) were size separated on a 12% Bis–Tris Gel (NuPAGE™, Invitrogen), and transferred to a PVDF membrane (iBlot ™, Invitrogen). Immunodetection was performed using antibodies directed against the EGFP tag and against endogenous Actin as a loading control (anti-EGFP, anti-Actin; Abcam). Immune complexes were detected by enhanced chemiluminescence (Lumi-Light^{PLUS}; Roche Applied Science). For analysis of plasma membrane targeting of fusion protein isoforms, the cell membrane component was first extracted (membrane protein extraction kit; BioVision) and then immunoblotted as described above. Immunoblotting with antibodies to endogenous Guanidinoacetate Methyl Transferase (GAMT) was used to confirm the purity of the extracted membrane fractions.

2.9. Fluorescence microscopy

Recombinant 3T3 Swiss cells seeded on glass slides (Menzel™ Superfrost) were fixed for 15 min at room temperature (RT) in 4% paraformaldehyde plus 1% Triton X-100 dissolved in phosphate buffered saline (PBS). Slides were washed and mounted for microscopy with Vectashield™ mounting medium (Vector Laboratories). Fluorescence was visualized at 63× magnification (Objective Plan-Apochromat 63×/ 1.40 oil) with a confocal microscope (LSM 510 Meta, Zeiss).

2.10. Transient transfection of HEK 293 cells

Kidney-derived HEK293 cells were cultured in 60 mm cell culture dishes under standard mammalian cell culture conditions to 40% confluence in DMEM cell culture medium (GIBCO, Scotland) supplemented with 1% pen/strep, 1% L-glutamine and 10% FBS. They were subsequently transfected (Fugene™ HD transfection reagent; Promega) with 10 μg of pEGFPN1-based *SLC6A8C* (CTR4), *SLC6A8D* (CTR5) or SLC19A3 (thiamine transporter) endotoxin-free plasmid DNA. All constructs were transfected in triplicate and the transfection efficiency based on EGFP fluorescence was estimated to be >90% in all plates (data not shown). 24 h after transfections, cell monolayers were washed, harvested with trypsin and seeded into 100 mm dishes to achieve a confluence of about 70% after 24 h in cell culture medium. 48 h after transfections, creatine uptake was performed as described in Section 2.7.

3. Results and discussion

3.1. Molecular identification and characterization of SLC6A8D

While cloning the *SLC6A8C* variant [14] from a HeLa cell line, a novel variant, which we named *SLC6A8D* (GenBank: KC800563), was discovered. This variant was the product of an in-frame deletion of exon 9, resulting in a novel 138 bp shorter form of the *SLC6A8C* mRNA (GenBank: EU280316). The rest of the sequence is 100% homologous to the *SLC6A8C* mRNA and its coding region is identical to that of *SLC6A8C* and *SLC6A8*. Thus at the protein level *SLC6A8D* (CTR5) is 100% homologous to *SLC6A8C* (CTR4) with the exception of a 46 amino acid in-frame deletion of residues 54 through 99. The deletion comprises the first cytosolic loop and the second transmembrane domain of the CTR4 protein (based on the LeuT model [19], Fig. 1). A pseudogene of *SLC6A8–SLC6A10P*, has been mapped to chr16 [20,21]. No *SLC6A8* PCR product was observed following a PCR on cDNA of a patient with a genomic deletion of the entire *SLC6A8* locus, using a forward primer complementary to both *SLC6A8* and *SLC6A10P* and a reverse primer specific to the 3′ UTR of *SLC6A8*. Furthermore, nested fragments of both *SLC6A8C* and *SLC6A8D* were amplified from PCR products of a forward primer in intron 4 and the *SLC6A8*–specific reverse primer. Taken together, these results confirm that *SLC6A8D* is a chrX transcript, and possesses identical 5′ and 3′ UTRs to those of *SLC6A8C* (Fig. 2).

3.2. Biological relevance of the SLC6A8D splice variant

In mouse we confirmed the expression of an exon 9-deficient variant (*Slc6a8d*) of *Slc6a8c*. *Slc6a8d* (GenBank: KC994641) expression was detected in transformed mouse embryonic fibroblasts (NIH-3T3 2.2) and, albeit at lower levels, in a mouse mammary gland cell line (NMuMG). For the first time we also show that *SLC6A8C* is expressed in monkey (Fig. 3).

3.3. Tissue-specific expression of SLC6A8, SLC6A8C and SLC6A8D

The expression levels of *SLC6A8* and its splice variants are highest in tissues with high energy requirement like the kidney, colon and small intestine (Fig. 4). Suggesting that like *SLC6A8*, the splice variants could

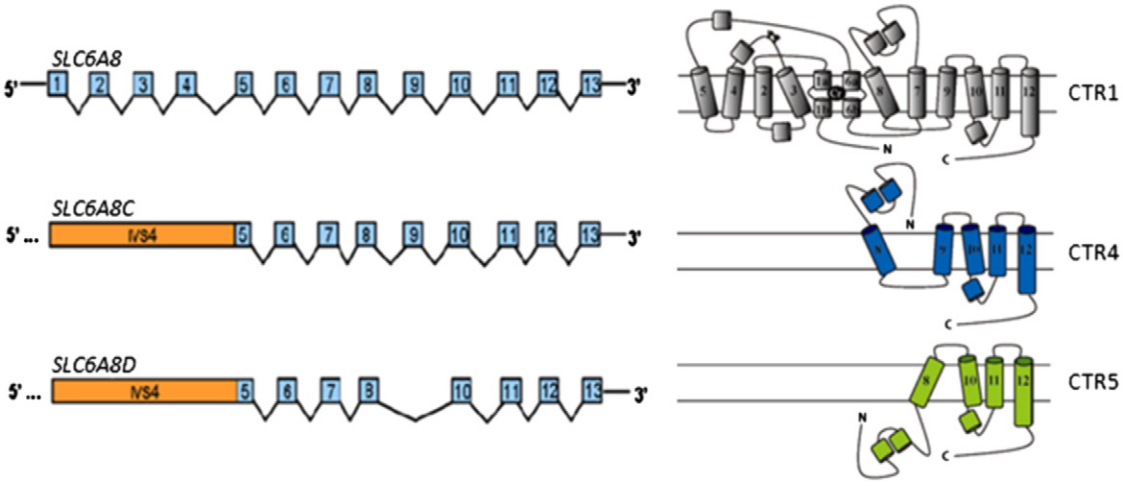

Fig. 1. Schematic representations *of SLC6A8*, *SLC6A8C* and *SLC6A8D* and their putative transmembrane domains. Because the exons, open reading frame and hence amino acids from *SLC6A8* are conserved with splicing, the last five (*SLC6A8C*) and last four (*SLC6A8D*) transmembrane domains are identical to those of the full length creatine transporter (CTR1). To be consistent with previous nomenclature, we refer to the *SLC6A8D* protein as CTR5.

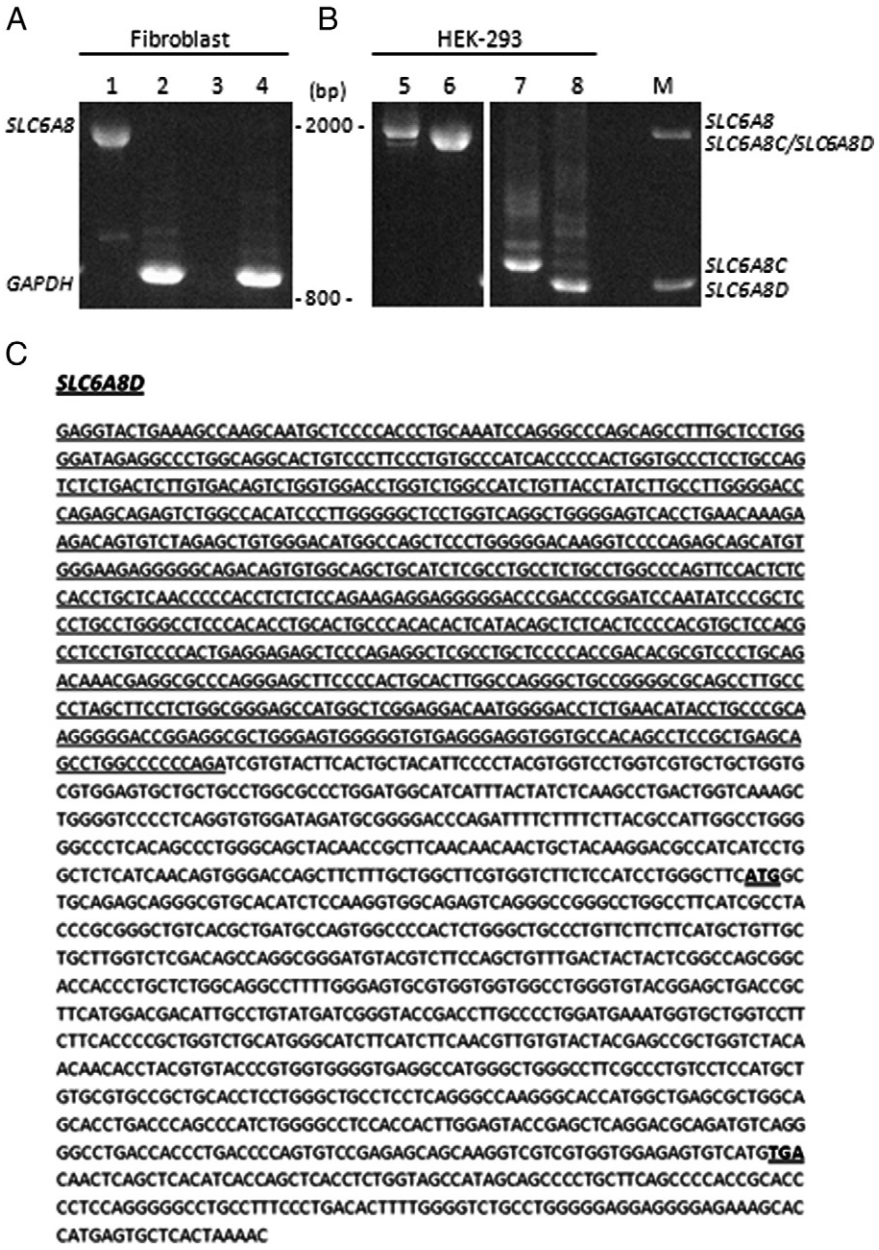

Fig. 2. Molecular characterization of *SLC6A8D*. (A) Shows specificity of reverse primer (Table 1, N_o. 4) to the *SLC6A8* transcript. No amplicon could be detected in fibroblasts from an individual with a genomic deletion encompassing the entire *SLC6A8* and its flanking genes (lanes 3 and 4) as opposed to control fibroblasts (lanes 1 and 2). This reverse primer in combination with an intron 4 forward primer was used to amplify both *SLC6A8C* and *SLC6A8D* messages (B) from HEK 293 cDNA (lane 6, primers; Table 1, N_o. 1). A nested PCR on the resulting amplicons with the same intron 4 forward primer and a reverse primer specific for either *SLC6A8C* (lane 7, primers; Table 1, N_o. 3) or *SLC6A8D* (lane 8, primers; Table 1, N_o. 2) confirms that the 5′UTR of *SLC6A8D* is at least as big as that of *SLC6A8C*. The mRNA sequence of *SLC6A8D*, as confirmed by sequencing of cloned PCR products from lane 6, is shown in (C). The underlined sequence depicts intron 4 of *SLC6A8*, while the bold printed nucleotides represent the cloned open reading frame of the *SLC6A8D* (CTR5) splice isoform. In all cell lines, absence of gDNA contamination was confirmed by PCR on cDNA synthesized without reverse transcriptase (data not shown).

also be involved in regulating creatine uptake. Across all 20 tissues tested, *SLC6A8C* is the most abundant splice variant of the two, with expression levels noticeably higher than that of *SLC6A8* in prostrate and thymus.

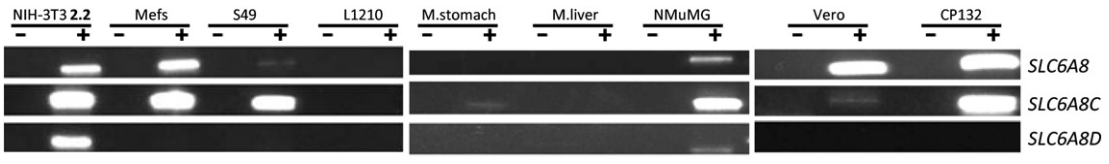

Fig. 3. Biological relevance of *SLC6A8D*. Expression of *SLC6A8D* was analyzed in several mouse cell lines (NIH-3T3 2.2, Mefs, S49, L1210) and tissues (stomach, liver) as well as in two monkey cell lines (Vero, CP132). Amplification of *SLC6A8*/*Slc6a8* and *SLC6A8C*/*Slc6a8c* as included controls. The reverse transcriptase (RTO) containing reactions are depicted by a + and the RTO negative reactions by a − character. Experiments were repeated at least three times and similar results were obtained: representative pictures are shown. *Slc6a8d* expression is only observed for the transformed fibroblasts (NIH-3T3 2.2) and the mammary epithelial cells (NMuMG).

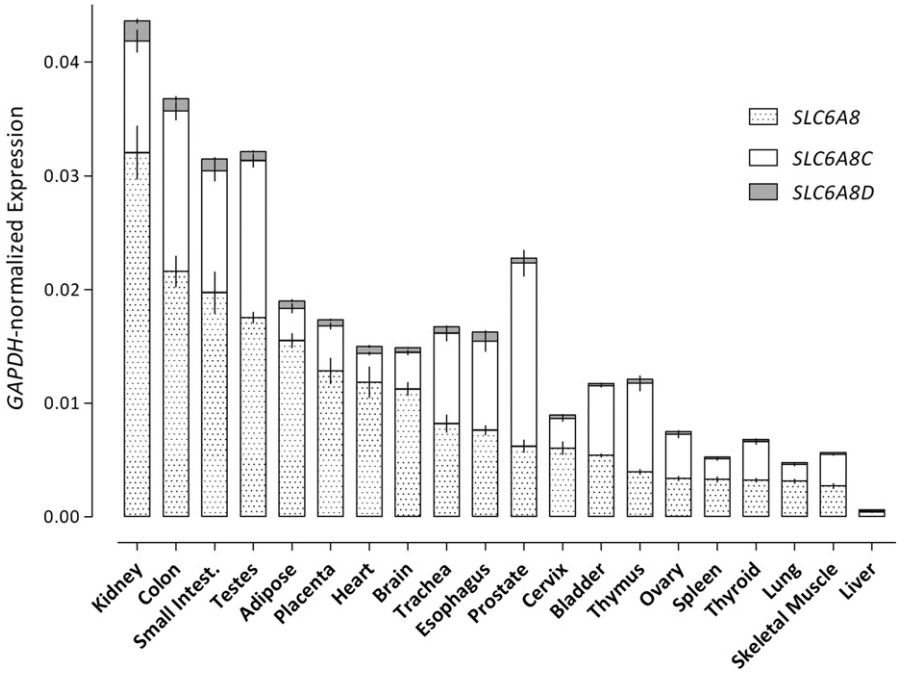

Fig. 4. Expression levels of *SLC6A8*, *SLC6A8C* and *SLC6A8D* across 20 human tissues. All target gene expression values were normalized using *GAPDH* as reference gene. Amplification efficiency of each primer pair (all between 98.22% and 99.91%) was determined by the standard curve method using serial dilutions of cDNA. The mean normalized expression is a function of the average C_T values of the target and reference genes respectively. Bars are mean ± SEM.

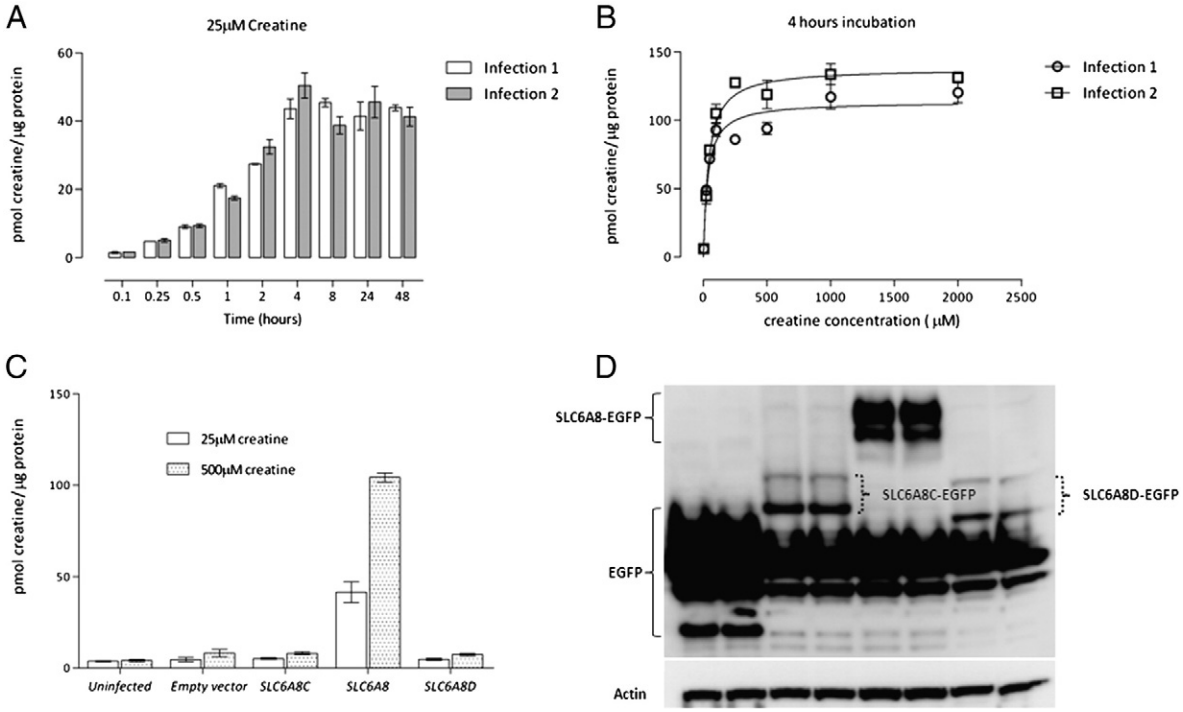

Fig. 5. Time course (A) and saturation kinetics (B) of creatine transport in recombinant 3T3 Swiss overexpressing *SLC6A8-EGFP*. Creatine uptake (on cells supplemented with 5, 25, 50, 100, 250, 500, 1000 and 2000 μM creatine) was performed as described in Section 2.7, in triplicate. Each bar represents the mean ± SEM. In the duplicate infections (I and II) uptake is linear within the first 4 h (A). Evaluation with a Michaelis–Menten model revealed a Vmax of 138 ± 3.8 and 113.3 ± 4.4 pmol/4 h/μg protein and a Km of 41.2 ± 5.5 and 34 ± 6.7 μM for Infections I and II respectively (B). Following overnight incubations, cells overexpressing the splice isoforms {*SLC6A8C* (CTR4) or *SLC6A8D* (CTR5)} accumulate similar levels of isotope-labeled creatine as those cells expressing only the empty vector or uninfected cells. On the other hand overexpression of *SLC6A8* (CTR1) results in a significantly higher creatine uptake capacity at both non-saturating (25 μM) and saturating (500 μM) creatine concentrations (C). Panel (D) shows the expression of EGFP fusion constructs in 40 μg of cell lysate. All cells were infected with two constructs using puromycin and hygromycin as co-selectable markers. "Empty vector" represents a combination of the pBPuro-EGFP/pBHygro-EGFP plasmids, "*SLC6A8C*" — the pBHygroEGFP/pBPuro-*SLC6A8C*-EGFP plasmids, "*SLC6A8*" — the pBHygroEGFP/pBPuro-*SLC6A8*-EGFP plasmids and "*SLC6A8D*" — the pBHygroEGFP/pBPuro-*SLC6A8C*-EGFP plasmids. To ensure that all lanes were loaded with equal amounts of protein, the blot was stripped and re-probed with an anti-actin antibody.

3.4. Splice variants SLC6A8C (CTR4) and SLC6A8D (CTR5) do not transport creatine

In recombinant *SLC6A8* cells (overexpressing CTR1) the time course for creatine uptake was linear for up to 4 h in both sets of infections (Fig. 5A). The saturation kinetics of creatine transport was determined following incubation in 5 μM–2 mM of creatine-[methyl-^{13}C]-supplemented medium for 4 h (Fig. 5B). Creatine transport followed Michaelis–Menten kinetics with Vmax values of 113.3 ± 4.4 and 138 ± 3.8 pmol/4 h/μg protein for infections I and II respectively, as well as Km values of 34 ± 6.7 μM (Infection I) and 41.2 ± 5.5 μM (Infection II). Following overnight incubations, cells overexpressing the splice isoforms accumulate similar levels of creatine-[methyl-^{13}C] compared to both cells expressing only the empty vector and uninfected cells. On the other hand overexpressing *SLC6A8* (CTR1) results in a 10 fold and a 13 fold increase in creatine uptake capacity at physiological (25 μM) and saturating (500 μM) creatine-[methyl-^{13}C] concentrations respectively (Fig. 5C). Expression of splice isoforms and the full length creatine transporter as a fusion to EGFP is confirmed on Western blot (Fig. 5D). Thus, the splice variants by themselves are not bonafide creatine transporters.

3.5. Re-infecting CTR1-expressing cells with either CTR4 (SLC6A8C) or CTR5 (SLC6A8D) upregulates creatine uptake at physiological concentrations, while increasing Vmax at saturating creatine concentrations

To explore whether the splice isoforms regulate *SLC6A8*, the transporter was expressed with or without additional expression of the splice variants, followed by analysis of creatine transport (Section 2.7). To rule out the possibility of passive creatine transport, a first set of incubations was carried out in medium supplemented only with creatine-[methyl-^{13}C] and in parallel a second set of incubations was carried out in a medium supplemented with equimolar amounts of creatine-[methyl-^{13}C] and guanidinopropionic acid (25, 500 and 1000 μM each). Guanidinopropionic acid (GPA) is a known competitive inhibitor of the creatine transporter [22]. Measurement of cellular creatine levels in the absence and presence of GPA shows that co-expression of the transporter with its splice variant enhances creatine uptake ($p < 0.05$) at both physiological (25 μM) and saturating (500 μM and 1000 μM) creatine concentrations. Decreased intracellular accumulation of creatine in the presence of GPA confirms that this enhanced uptake is not due to passive diffusion of creatine into the cells (Fig. 6 and 6B). We observe an increase in the maximum rate of creatine transport

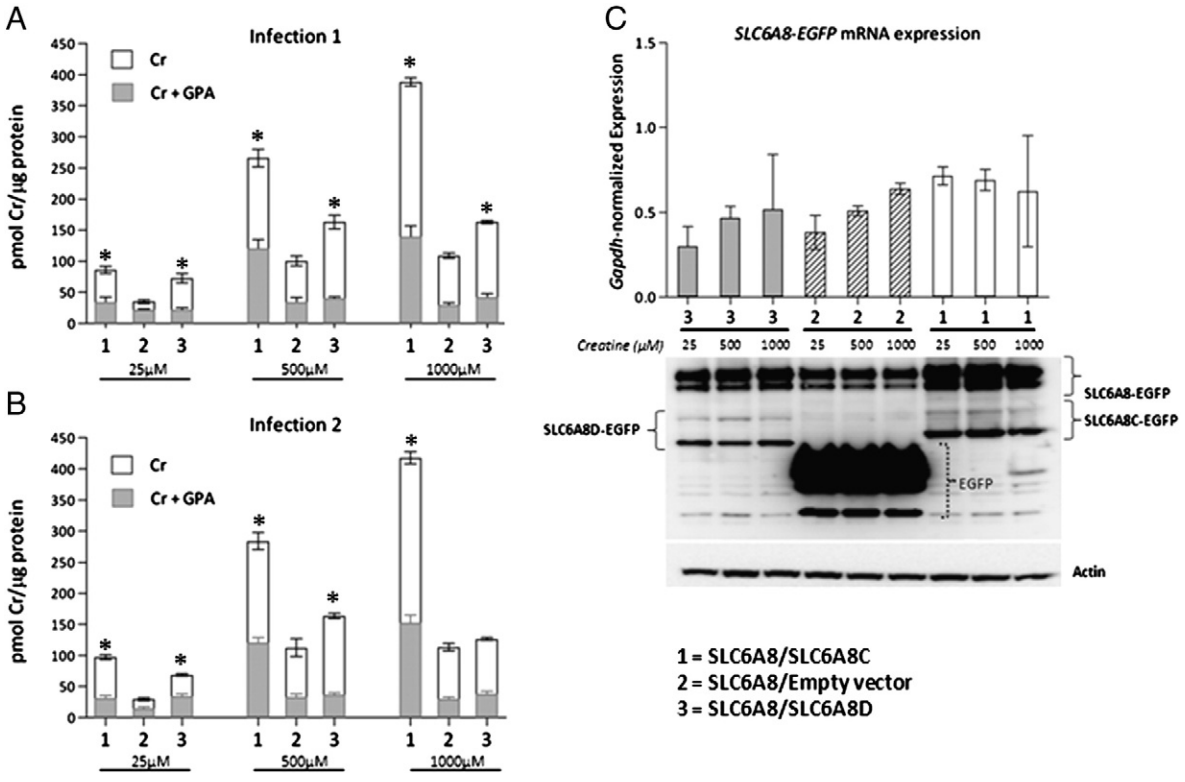

Fig. 6. Upregulated creatine transport due to increased *SLC6A8* protein (CTR1) levels in 3T3 Swiss-*SLC6A8* cells re-infected with *SLC6A8C* or *SLC6A8D*. Infection I (A, upper panel) and Infection II (B, lower panel) represent independent secondary infections of each construct (empty vector, *SLC6A8C* or *SLC6A8D*) on cells already overexpressing *SLC6A8-EGFP*. Incubations were carried out in triplicate and the measured intracellular creatine was normalized to the total protein content. Cells were incubated with only creatine (Cr) or with equimolar amounts of creatine and guanidino propionic acid (Cr + GPA). Each bar represents the mean ± SEM, and * a p value < 0.05 (one-way ANOVA followed by Dunnett's post-test, comparing *SLC6A8*/empty vector to either *SLC6A8*/*SLC6A8C* or *SLC6A8*/*SLC6A8D* using the GraphPad Prism software). At non-saturating creatine concentrations (25 μM), creatine transport is significantly upregulated 2–3 fold in *SLC6A8*/*SLC6A8C* and *SLC6A8*/*SLC6A8D* cells when compared to cells expressing only *SLC6A8* and the empty vector (*SLC6A8*/empty vector). At saturating creatine concentrations (500 and 1000 μM), the same holds true for the *SLC6A8*/*SLC6A8C* cell lines (up to 4 fold increase); however the upregulation (10–60% increase) is lower in the *SLC6A8*/*SLC6A8D* cells when compared to the *SLC6A8*/empty vector cell lines. To determine if this enhanced creatine accumulating capacity following addition of a splice variant was due to increased *SLC6A8* transcription/translation and hence the amount of transporter available at the plasma membrane, quantitative real time PCR was carried out on cell pellets from Infection I (C, upper panel). The normalized expression is a function of the average C_T values of *SLC6A8-EGFP* and mouse *Gapdh* respectively. Bars are mean ± SEM. There is no significant difference in recombinant *SLC6A8-EGFP* mRNA expression between 3T3 Swiss-*SLC6A8* cells co-expressing a splice variant and those co-expressing the empty vector. However on a Western blot (C, lower panel) *SLC6A8* protein levels (CTR1) are higher when either the *SLC6A8C* (CTR4) or *SLC6A8D* (CTR5) isoform was co-expressed in place of the empty vector. CTR4 protein levels are higher than those of CTR45 (possibly resulting from higher transfection efficiencies and as such a higher viral titer) with a corresponding higher expression of CTR1. Re-probing the same blot with an anti-actin antibody was carried out as a loading control.

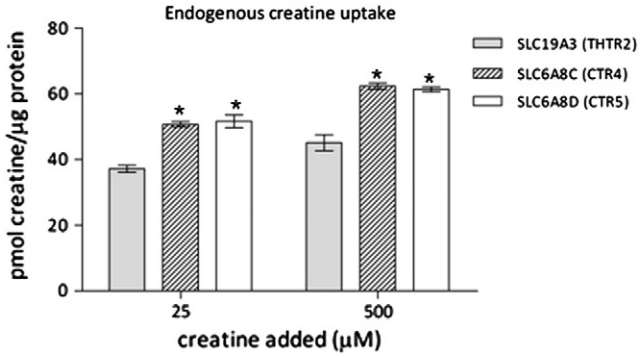

Fig. 7. Physiological relevance of splice variants on endogenous CTR1 in HEK293 cells. Creatine transport is significantly increased by 26–28% in HEK293 cells overexpressing the CTR4 or CTR5 splice isoform compared to cells overexpression the thiamine transporter (SLC19A3). * indicates p value < 0.001 (one-way ANOVA followed by Dunnett's post-test — GraphPad Prism software) between effect on endogenous creatine transport due to CTR4/CTR5 compared to SLC19A3. The uptake of creatine in cells overexpressing SLC19A3 (THTR2) was 8% reduced compared to the pEGFPN1 (empty vector) transfectants (data not shown), which is most likely explained by the fact that the cells have more difficulties in expressing a membrane protein than EGFP only.

following addition of *SLC6A8C* or *SLC6A8D* as opposed to addition of the empty vector, in recombinant *SLC6A8*-expressing cells. At non-saturating creatine concentrations (25 μM) the extent to which *SLC6A8D* enhances creatine transport is comparable to that by *SLC6A8C* (2–3 fold). On the other hand at saturating substrate concentrations (500/1000 μM) the maximum *SLC6A8D*-mediated increase in creatine uptake was only about 1.5 fold as opposed to a 4 fold increase in the case of *SLC6A8C*. This is most likely due to the higher expression of CTR4 (*SLC6A8C-EGFP*) compared to CTR5 (*SLC6A8D-EGFP*) (Fig. 6C, lower panel), resulting in higher CTR1 (*SLC6A8-EGFP*) protein levels and a concomitant increase in creatine uptake capacity.

3.6. Physiological relevance ofCTR4 and CTR5

To confirm that the splice variants increase the creatine uptake mediated by the endogenous creatine transporter we transiently transfected the kidney-derived HEK293 cells with a pEGFPN1 based *SLC6A8C* (CTR4) or *SLC6A8D* (CTR5) plasmid. As a control to exclude that overexpression of an unrelated transporter would give a similar effect we also transiently transfected a pEGFPN1 based SLC19A3 (thiamine transporter) construct. Their effect on endogenous creatine uptake was determined as described in Section 2. At both 25 μM and 500 μM creatine concentrations HEK293 cells overexpressing CTR4 and CTR5 had a significant increase (p value < 0.005) in creatine transport compared to cells over-expressing SLC19A3. Though moderate (around 25% increase), the increase of creatine uptake following overexpression of CTR4 and CTR5 in HEK293 cells is in line with what is observed for the heterologous mouse 3T3 Swiss expression system (Fig. 7). This confirms that overexpression of the splice variants has a positive effect on the function of the endogenously expressed creatine transporter.

3.7. Splice-variant-dependent upregulation of creatine transport by CTR1 occurs at post transcription

After depletion of intracellular creatine followed by incubation in 25, 500 and1000 μM creatine-[methyl-^{13}C]-supplemented medium for 4 h, *SLC6A8-EGFP* mRNA levels were evaluated in recombinant *SLC6A8* cells additionally expressing the empty vector or a splice isoform. At both physiological and saturating creatine concentrations there is no significant difference in *SLC6A8* (*SLC6A8-EGFP*) transcription in the *SLC6A8*/empty vector cell line compared to the *SLC6A8*/*SLC6A8C* or *SLC6A8*/*SLC6A8D* cell lines (Fig. 6C, upper panel). A Western blot (Fig. 6C, lower panel) shows bands at 100 kDa and 90 kDa corresponding to the glycosylated and unglycosylated *SLC6A8-EGFP* fusion proteins. There are also bands at 50 kDa (*SLC6A8C-EGFP*), 40 kDa (*SLC6A8D-EGFP*) and 25 kDa (*EGFP*). Western blotting reveals that expression of CTR1 (*SLC6A8-EGFP*) compared to Actin levels is lower in the absence of a co-expressed splice isoform. Interestingly, expression of CTR4 (*SLC6A8C-EGFP*) is higher than CTR5 (*SLC6A8D-EGFP*) with a corresponding higher co-expression of CTR1. Thus, additional expression of either CTR4 or CTR5 to CTR1-expressing cells results in an increase in total CTR1 levels. This splice-variant-associated increase in CTR1 protein levels was not accompanied by an increase in mRNA levels, suggesting (post)translational rather than transcriptional regulation. This positive regulation of a parent transporter by its otherwise non-functional variant is of great interest as previous reports investigating the functional relevance of splicing among neurotransmitter transporters revealed a dominant negative effect of the splice isoforms on the function of the transporter. Co-expression of a non-functional rat norepinephrine transporter splice isoform (rNETb) with a functional rNETa isoform in COS cells, decreased the expression and hence activity of the rNETa

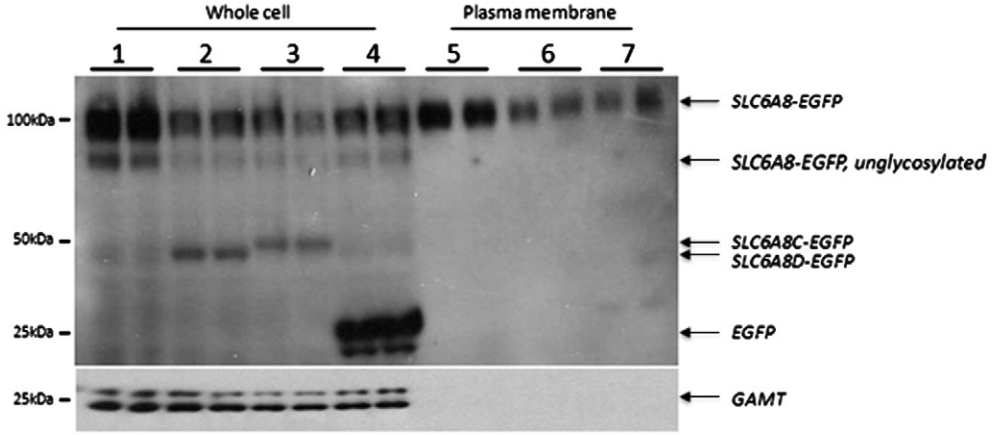

Fig. 8. Localization of EGFP fusion constructs. To investigate if fusion proteins are targeted to the plasma membrane, 3T3 Swiss-*SLC6A8*, -*SLC6A8*/empty vector, -*SLC6A8*/*SLC6A8C* and -*SLC6A8*/*SLC6A8D* cells were incubated in 25 μM creatine overnight. A whole cell fraction (lanes 1–4) and a plasma membrane fraction (lanes 5–7) of each recombinant cell type were analyzed on a Western blot. Whole cell fractions were loaded as follows: lane 1; *SLC6A8*, lane 2; *SLC6A8*/*SLC6A8D*, lane 3; *SLC6A8*/*SLC6A8C*, lane 4; *SLC6A8*/Empty vector. Lanes 5, 6 and 7 are plasma membrane fractions of the samples in lanes 2, 3 and 4 respectively. An antibody directed against cytosolic guanidinoacetate N-methyl transferase (GAMT) was used to confirm the purity of the plasma membrane fraction. The Western blots show that, of all fusion proteins, only *SLC6A8-EGFP* (CTR1) is targeted to the plasma membrane. Absence of the GAMT protein and the unglycosylated *SLC6A8-EGFP* (glycosylation of the creatine transporter occurs at the Golgi before it is targeted to the plasma membrane, thus these unglycosylated moieties are most likely its ER–Golgi intermediates [44]) confirms the purity of the plasma membrane fractions.

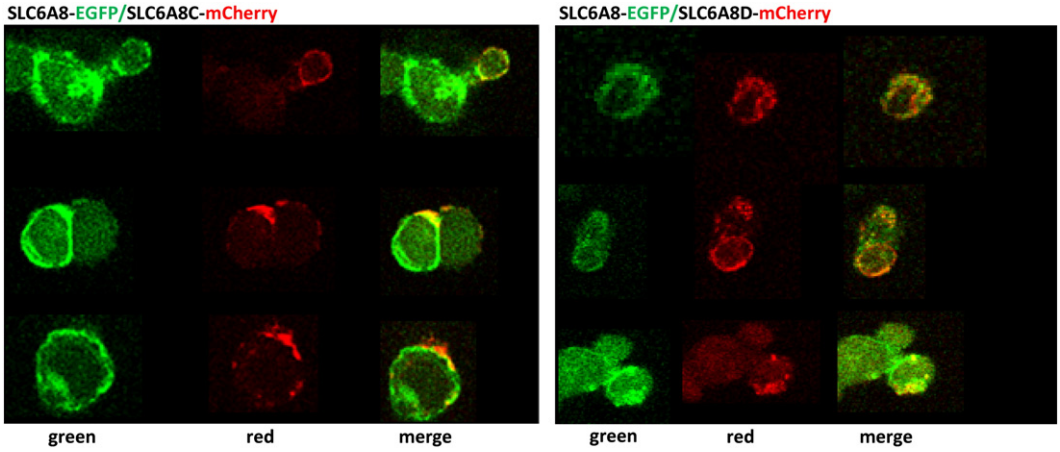

Fig. 9. Co-localization of CTR1 with CTR4 and CTR5. Confocal image acquisition (Objective Plan-Apochromat 63×/1.40 oil; LSM 510 Meta, Zeiss) of cells co-expressing *SLC6A8-EGFP* (CTR1) and *SLC6A8C*-mCherry (CTR4) or *SLC6A8D*-mCherry (CTR5) indicates that the full length transporter co-localizes with its truncated splice isoforms.

isoform [23]. A similar scenario has been described for the glutamate-transporting EAAT1 transporter and its EAAT1exon9skip splice variant [24]. This is very interesting as it raises the possibility that although the regulatory mechanisms in this family of transporters seem to be conserved, the effect on protein function may be different.

3.8. Splice isoforms may facilitate endoplasmic reticulum exit and/or trafficking of full-length transporter

Purification of the plasma membrane (PM) fraction of recombinant 3T3 Swiss cells shows that the splice variants are not localized to the plasma membrane like CTR1 (Fig. 8). Thus the splice isoforms do not internalize together with the full-length transporter at the PM to facilitate or enhance its affinity for creatine. However, by replacing the EGFP tag on CTR4 and CTR5 with mCherry (*SLC6A8C*-mCherry and *SLC6A8D*-mCherry respectively), we show that both CTR4 and CTR5 co-localize with CTR1 (Fig. 9). It is plausible that the splice variants do oligomerize to CTR1 at the level of the ER to facilitate its trafficking to the Golgi, where it will undergo further modification(s) before being targeted to the plasma membrane. This is consistent with previous studies involving regulation of Na^+/Cl^- cotransporters and further emphasizes the notion that oligomerization-dependent regulation seems to be common among members of this transporter family [25,26].

4. Concluding remarks

In this study we identified a novel variant of *SLC6A8–SLC6A8D*; identical to *SLC6A8C*, but lacking exon 9. Differential expression between tissues and conservation across species suggested a functional relevance of these variants. Functional creatine transport analyses reveal that although these splice isoforms do not transport creatine, their co-expression with the full-length transporter results in an enhanced capacity for creatine uptake, reflected by an increase in protein expression of the creatine transporter. Varying the cell surface levels of the transporter via altered trafficking is a fairly common avenue for regulation of neurotransmitter transporters. This results in the maximum rate of transporter activity (Vmax) being altered with little to no change in substrate affinity (Km), reviewed in [27,28]. Studies investigating changes in creatine transporter levels in response to extracellular creatine have shown that creatine saturation or depletion was associated with a reduced or increased Vmax respectively, of creatine transport. In these studies, changes in plasma membrane rather than total CTR1 levels resulted in the altered Vmax [29–33]. The increase in total CTR1 levels in our case, following addition of a splice isoform is an indication that besides being involved in CTR1 trafficking, these splice isoforms may also be involved in extending the half-life of the mature transporter. A possible avenue could be via the ubiquitin-protein ligase — Nedd4-2 (neuronal precursor cell expressed developmentally down-regulated protein), which targets a number of membrane proteins including receptors and ion channels for degradation by the proteasome. A Nedd-4-2-mediated decrease in plasma membrane levels has been shown for the dopamine [34], glucose [35], glutamate [36,37] and thiazide-sensitive [38] Na^+/Cl^- cotransporters, suggesting that this mechanism could be relevant for regulating the Na^+/Cl^- creatine transporter as well. In fact there is evidence that the serum/glucocorticoid-regulated kinases (SGK1 and SGK3), which are inhibitors of Nedd4-2 [38–42] increase the maximal transport rate of CTR1 [43]. For the moment we can only speculate that by virtue of their homology to the full-length transporter, *SLC6A8C* (CTR4) and *SLC6A8D* (CTR5) can act as alternative targets and thus insulate the transporter from ubiquitin ligases. The extent and nature of this regulation of *SLC6A8* by *SLC6A8C* and *SLC6A8D* is subject to future investigations. Their effect of enhancing creatine accumulation by *SLC6A8* provides new avenues to explore the regulation of the creatine transporter, which may also be relevant for other members of this transporter family.

Acknowledgements

The authors are grateful to Herman ten Brink for synthesis of the creatine-[methyl-^{13}C]. The anti-GAMT antibodies were a kind gift from Theo Walliman's lab. The mCherry plasmid was obtained by courtesy of Roger Tsien's lab.

References

[1] J. Gécz, C. Shoubridge, M. Corbett, The genetic landscape of intellectual disability arising from chromosome X, Trends Genet. 25 (2009) 308–316.
[2] G.S. Salomons, S.J. van Dooren, N.M. Verhoeven, K.M. Cecil, W.S. Ball, T.J. Degrauw, et al., X-linked creatine-transporter gene (SLC6A8) defect: a new creatine-deficiency syndrome, Am. J. Hum. Genet. 68 (2001) 1497–1500.
[3] C.B. Item, S. Stöckler-Ipsiroglu, C. Stromberger, A. Mühl, M.G. Alessandrì, M.C. Bianchi, et al., Arginine:glycine amidinotransferase deficiency: the third inborn error of creatine metabolism in humans, Am. J. Hum. Genet. 69 (2001) 1127–1133.
[4] S. Stöckler, D. Isbrandt, F. Hanefeld, B. Schmidt, K. von Figura, Guanidinoacetate methyltransferase deficiency: the first inborn error of creatine metabolism in man, Am. J. Hum. Genet. 58 (1996) 914–922.
[5] S. Stöckler-ipsiroglu, G.S. Salomons, Inborn metabolic diseases: diagnosis and treatment, Mol. Cell. Biochem. 244 (2006) 211–217.
[6] M. Wyss, R. Kaddurah-Daouk, Creatine and creatinine metabolism, Physiol. Rev. 80 (2000) 1107–1213.
[7] A. Evangeliou, K. Vasilaki, P. Karagianni, N. Nikolaidis, Clinical applications of creatine supplementation on paediatrics, Curr. Pharm. Biotechnol. 10 (2009) 683–690.
[8] A.M. Klein, R.J. Ferrante, The neuroprotective role of creatine, Subcell. Biochem. 46 (2008) 205–243.

[9] J. Wallis, C.A. Lygate, A. Fischer, M. ten Hove, J.E. Schneider, L. Sebag-Montefiore, et al., Supranormal myocardial creatine and phosphocreatine concentrations lead to cardiac hypertrophy and heart failure: insights from creatine transporter-overexpressing transgenic mice, Circulation 112 (2005) 3131–3139.
[10] A.J. Lopez, Alternative splicing of pre-mRNA: developmental consequences and mechanisms of regulation, Annu. Rev. Genet. 32 (1998) 279–305.
[11] D.L. Black, Protein diversity from alternative splicing: a challenge for bioinformatics and post-genome biology, Cell 103 (2000) 367–370.
[12] B. Modrek, C. Lee, A genomic view of alternative splicing, Nat. Genet. 30 (2002) 13–19.
[13] E.T. Wang, R. Sandberg, S. Luo, I. Khrebtukova, L. Zhang, C. Mayr, et al., Alternative isoform regulation in human tissue transcriptomes, Nature 456 (2008) 470–476.
[14] C. Martínez-Muñoz, E.H. Rosenberg, C. Jakobs, G.S. Salomons, Identification, characterization and cloning of SLC6A8C, a novel splice variant of the creatine transporter gene, Gene 418 (2008) 53–59.
[15] P. Simon, Q-Gene: processing quantitative real-time RT-PCR data, Bioinformatics 19 (2003) 1439–1440.
[16] P.Y. Muller, A.R. Miserez, Z. Dobbie, Processing of gene expression data generated by quantitative real-time RT-PCR, BioTechniques 32 (2002) 1–6.
[17] E.H. Rosenberg, C. Martínez Muñoz, O.T. Betsalel, S.J. van Dooren, M. Fernandez, C. Jakobs, et al., Functional characterization of missense variants in the creatine transporter gene (SLC6A8): improved diagnostic application, Hum. Mutat. 28 (2007) 890–896.
[18] C. Amat di San Filippo, N. Longo, Tyrosine residues affecting sodium stimulation of carnitine transport in the OCTN2 carnitine/organic cation transporter, J. Biol. Chem. 279 (2004) 7247–7253.
[19] A. Yamashita, S.K. Singh, T. Kawate, Y. Jin, E. Gouaux, Crystal structure of a bacterial homologue of Na^+/Cl^- dependent neurotransmitter transporters, Nature 437 (2005) 215–223.
[20] G.S. Iyer, R. Krahe, L.A. Goodwin, N.A. Doggett, M.J. Siciliano, V.L. Funanage, et al., Identification of a testis-expressed creatine transporter gene at 16p11.2 and confirmation of the X-linked locus to Xq28, Genomics 34 (1996) 143–146.
[21] E.E. Eichler, F. Lu, Y. Shen, R. Antonacci, V. Jurecic, N.A. Doggett, et al., Duplication of a gene-rich cluster between 16p11.1 and Xq28: a novel pericentromeric-directed mechanism for paralogous genome evolution, Hum. Mol. Genet. 5 (1996) 899–912.
[22] A. Möller, B. Hamprecht, Creatine transport in cultured cells of rat and mouse brain, J. Neurochem. 52 (1989) 544–550.
[23] S. Kitayama, Dominant negative isoform of rat norepinephrine transporter produced by alternative RNA splicing, J. Biol. Chem. 274 (1999) 10731–10736.
[24] A. Vallejo-Illarramendi, M. Domercq, C. Matute, A novel alternative splicing form of excitatory amino acid transporter 1 is a negative regulator of glutamate uptake, J. Neurochem. 95 (2005) 341–348.
[25] H. Sitte, Oligomer formation by Na^+–Cl^--coupled neurotransmitter transporters, Eur. J. Pharmacol. 479 (2003) 229–236.
[26] H.H. Sitte, H. Farhan, J.A. Javitch, Sodium-dependent neurotransmitter transporters: oligomerization as a determinant of transporter function and trafficking, Mol. Interv. 4 (2004) 38–47.
[27] G.E. Torres, S.G. Amara, Glutamate and monoamine transporters: new visions of form and function, Curr. Opin. Neurobiol. 17 (2007) 304–312.
[28] A.S. Kristensen, J. Andersen, T.N. Jørgensen, L. Sørensen, J. Eriksen, C.J. Loland, et al., SLC6 neurotransmitter transporters: structure, function, and regulation, Pharmacol. Rev. 63 (2011) 585–640.
[29] E. Boehm, S. Chan, M. Monfared, T. Wallimann, K. Clarke, S. Neubauer, Creatine transporter activity and content in the rat heart supplemented by and depleted of creatine, Am. J. Physiol. Endocrinol. Metab. 284 (2003) E399–E406.
[30] J.J. Brault, K.A. Abraham, R.L. Terjung, Muscle creatine uptake and creatine transporter expression in response to creatine supplementation and depletion, J. Appl. Physiol. 94 (2003) 2173–2180.
[31] M.D. Darrabie, A.J.L. Arciniegas, R. Mishra, D.E. Bowles, D.O. Jacobs, L. Santacruz, AMPK and substrate availability regulate creatine transport in cultured cardiomyocytes, Am. J. Physiol. Endocrinol. Metab. 300 (2011) E870–E876.
[32] J.D. Loike, D.L. Zalutsky, E. Kaback, A.F. Miranda, S.C. Silverstein, Extracellular creatine regulates creatine transport in rat and human muscle cells, Proc. Natl. Acad. Sci. U. S. A. 85 (1988) 807–811.
[33] M. Tarnopolsky, G. Parise, M.-H. Fu, A. Brose, A. Parshad, O. Speer, et al., Acute and moderate-term creatine monohydrate supplementation does not affect creatine transporter mRNA or protein content in either young or elderly humans, Mol. Cell. Biochem. 244 (2003) 159–166.
[34] T. Sorkina, M. Miranda, K.R. Dionne, B.R. Hoover, N.R. Zahniser, A. Sorkin, RNA interference screen reveals an essential role of Nedd4-2 in dopamine transporter ubiquitination and endocytosis, J. Neurosci. 26 (2006) 8195–8205.
[35] M. Dieter, M. Palmada, Regulation of glucose transporter SGLT1 by ubiquitin ligase Nedd4-2 and kinases SGK1, SGK3, and PKB, Obes. Res. 5 (2004) 862–870.
[36] C. Boehmer, G. Henke, Regulation of the glutamate transporter EAAT1 by the ubiquitin ligase Nedd4-2 and the serum and glucocorticoid-inducible kinase isoforms SGK1/3 and protein kinase B, J. Neurochem. 86 (2003) 1181–1188.
[37] C. Boehmer, Post-translational regulation of EAAT2 function by co-expressed ubiquitin ligase Nedd4-2 is impacted by SGK kinases, J. Neurochem. 97 (2006) 911–921.
[38] J. Arroyo, D. Lagnaz, Nedd4-2 modulates renal Na^+–Cl^- cotransporter via the aldosterone–SGK1–Nedd4-2 pathway, J. Am. Soc. Nephrol. 22 (2011) 1707–1719.
[39] P. Snyder, D. Olson, B. Thomas, Serum and glucocorticoid-regulated kinase modulates Nedd4-2-mediated inhibition of the epithelial Na^+ channel, J. Biol. Chem. 4 (2002) 5–8.
[40] P. Snyder, D. Olson, R. Kabra, cAMP and serum and glucocorticoid-inducible kinase (SGK) regulate the epithelial Na^+ channel through convergent phosphorylation of Nedd4-2, J. Biol. Chem. 29 (2004) 45753–45758.
[41] B. Friedrich, Y. Feng, P. Cohen, T. Risler, The serine/threonine kinases SGK2 and SGK3 are potent stimulators of the epithelial Na^+ channel α, β, γ-ENaC, Pflugers Arch.-Eur. J. Physiol. 445 (2003) 693–696.
[42] V. Bhalla, D. Daidié, H. Li, Serum- and glucocorticoid-regulated kinase 1 regulates ubiquitin ligase neural precursor cell-expressed, developmentally down-regulated protein 4-2 by inducing interaction with 14-3-3, Mol. Endocrinol. 19 (2005) 3073–3084.
[43] M. Shojaiefard, D.L. Christie, F. Lang, Stimulation of the creatine transporter SLC6A8 by the protein kinases SGK1 and SGK3, Biochem. Biophys. Res. Commun. 334 (2005) 742–746.
[44] N. Straumann, A. Wind, T. Leuenberger, T. Wallimann, Effects of N-linked glycosylation on the creatine transporter, Biochem. J. 393 (2006) 459–469.
[45] O. Braissant, H. Henry, E. Béard, J. Uldry, Creatine deficiency syndromes and the importance of creatine synthesis in the brain, Amino Acids 40 (5) (2011) 1315–1324.